Journal of the European Ceramic Society 22 (2002) 603–612

www.elsevier.com/locate/jeurceramsoc

Ostwald ripening kinetics of angular grains dispersed in a liquid phase by two-dimensional nucleation and abnormal grain growth

Muyung-Koo Kang[a], Doh-Yeon Kim[a], Nong M. Hwang[a,b,*]

[a]*Center for Microstructure Science of Materials, School of Materials Science and Engineering, Seoul National University, Seoul 151-742, South Korea*

[b]*Korea Research Institute of Standards and Science, PO Box 102, Taejon, 305-600, South Korea*

Received 21 March 2001; accepted 20 May 2001

Abstract

Based on the fact that the angular shape of solid grains dispersed in the liquid matrix indicates a singular interface, the coarsening kinetics of angular grains was formulated based on 2-dimensional (2-D) nucleation and solved numerically. For comparison, diffusion-controlled coarsening of grains with a spherical shape was also solved numerically. The solutions showed that coarsening by 2-D nucleation induced abnormal grain growth whilst diffusion-controlled coarsening did not. This result agrees with the general experimental observation that the abnormal grain growth in liquid phase sintering takes place exclusively in the system with angular grains. The ratio of the largest grain size to the average increased monotonously with time in coarsening by 2-D nucleation whilst it decreased in diffusion-controlled coarsening. The artificially-added large grain (10 times larger than the average) became the abnormal grain in 2-D nucleation controlled coarsening but did not in diffusion-controlled coarsening.

Keywords: Abnormal grain growth; Grain growth; Interface structure; Liquid phase sintering; Nucleation; Simulation

1. Introduction

In liquid-phase sintered materials, solid grains dispersed in a liquid matrix undergo coarsening during heat-treatment. Coarsening is driven by a reduction of the total solid/liquid interface (S/L) area. Larger grains grow at the expense of smaller ones with a total volume of solid grains conserved; the phenomenon is called Ostwald ripening.[1] The growth kinetics of diffusion-controlled Ostwald ripening is relatively well established; Lifshitz and Slyozov[2] and Wagner[3] (LSW) formulated the phenomenon and obtained the analytical solution. The modified LSW (MLSW) theory[4] treated a more realistic case with an appreciable volume fraction of solid. These treatments showed that the average size increases in proportion to a cube root of time and that the normalized grain size distribution is stationary. This type of coarsening is called normal grain growth in comparison with abnormal grain growth (AGG), where a few grains undergo exclusive growth compared to other grains. The term ''abnormal grain growth'' is also referred to the case of single phase systems such as Fe–3%Si.[5] In this case, grain growth occurs by migration of grain boundaries while Ostwald ripening occurs by solution and reprecipitation process. To our knowledge, the mechanism of AGG in single phase sytems[6] is different from that of AGG in two phase systems which is a topic of this paper.

There are two types of equilibrium shape of solid grains in a liquid matrix: spherical and angular. Atomic structures of the interface for spherical and angular grains are well established. For example, Jackson[7] showed that the atomic structure of the interface is classified into the entropy-dominant disordered and the enthalpy-dominant ordered one. The former and the latter are called rough and singular interfaces, respectively. The energy of a rough interface is isotropic while that of a singular interface is anisotropic. As a result, the equilibrium shape of a grain with a rough interface is spherical while that with a singular interface is angular.

In general agreement with Jackson's α parameter[7] for the singular-rough interface transition, systems with solid grains of relatively weak metallic bonding tend to

* Corresponding author. Tel.: +82-2-880-8922; fax: +82-2-882-8164.

E-mail address: nmhwang@kriss.re.kr (N.M. Hwang).

0955-2219/02/$ - see front matter
PII: S0955-2219(01)00370-3

have spherical grains in a liquid matrix while systems with solid grains of relatively strong covalent or ionic bonding tend to have angular ones. For example, solid grains are spherical in liquid phase sintering of metallic systems, Co–Cu,[8] Fe–Cu,[8] W–Ni,[9] and Mo–Ni.[10] On the other hand, solid grains are angular in carbide systems such as WC-Co,[11] TaC–Co,[12] VC–Co,[12] B_4C[13] and SiC,[14] in oxide systems such as Al_2O_3,[15] $BaTiO_3$,[16] ferrite,[17,18] yttrium barium copper oxide (YBCO) superconductors,[19,20] and mullite[21] and in nitride systems such as Si_3N_4.[22,23] There are some exceptions for this trend. For example, MgO grains in $CaMgSiO_4$ are spherical.[24]

Even if the equilibrium shape of a grain is spherical, it can be anhedral when dispersed in a small amount of the liquid phase. In the extreme case, the liquid phase exists as a thin liquid film. Then, the interface structure of solid grains may be difficult to determine. Even in this case, however, the growing grains with a singular interface tend to be enclosed by the surface with the slowest growing direction, leading to straight interfaces. On the other hand, the growing grains with a rough interface are round at least at the corners and have much less tendency to have straight interfaces. Normally, coarsening of spherical grains is diffusion-controlled[8–10] and that of angular grains is interface-controlled.[12,25,26] To our knowledge, coarsening of spherical grains shows normal grain growth without exceptions, which is in agreement with the analysis by LSW or MLSW. However, coarsening of angular grains often leads to AGG.[11–23]

The kinetics of atomic attachment to the interface is quite different between the two interfaces.[27–29] The rough interface is full of kink sites and there is no barrier to atomic attachment. This leads to diffusion-controlled growth. The singular interface lacks kink or ledge sites and for atomic attachment, ledge-generating sources such as screw dislocation or two-dimensional (2-D) nucleation are needed; typically, the growth is interface controlled.

Although growth by 2-D or screw dislocation is well established in a crystal growth theory,[27–29] the concept was rarely used in coarsening of the angular grains dispersed in a liquid matrix. Angular grains are very common in ceramics as well as in hard metals such as WC–Co. Therefore, understanding the coarsening kinetics of angular grains is necessary. Herring[30] has suggested in his classical paper that the growth of a facet plane would require a 2-D nucleation process. Therefore, he tacitly explained AGG by suggesting a discontinuous variation in coarsening behavior when coarsening was by 2-D nucleation. Furthermore, Wynblatt et al.[31,32] showed that the "nucleation inhibited" growth of faceted particles could account satisfactorily for the coarsening of Pt particles on flat alumina substrates. Although they did not explicitly mention the AGG behavior during liquid-phase sintering, their works are believed to lay a firm base for the 2-D nucleation controlled coarsening process.

In order to understand the coarsening kinetics of angular grains dispersed in the liquid phase, the differential equation describing the coarsening rate based on screw dislocation or 2-D nucleation must be solved simultaneously with the mass conservation equation during the dissolution of shrinking grains and reprecipitation on growing grains. However, the resulting partial differential equations have too complicated forms to obtain an analytical solution. In this paper a numerical solution for coarsening by 2-D nucleation is reported. The results for screw dislocation are described in the reference.[33]

On the other hand, many experimental results related to AGG supported coarsening by 2-D nucleation.[11,34–37] These results imply that coarsening by 2-D nucleation might be responsible for AGG in many ceramic systems as well as in some metallic systems of faceted grains dispersed in the liquid phase. 2-D nucleation depends exponentially on the driving force. Therefore, only certain grains with a capillary driving force high enough to trigger the 2-D nucleation would grow. The growth of other grains will be suppressed, which might be the condition for AGG. In this paper, we focused on the possibility that the numerical solution for coarsening of angular grains by 2-D nucleation should lead to AGG.

2. Coarsening by 2-D nucleation and procedure for numerical solution

In order for coarsening to take place by 2-D nucleation, the 2-D nucleation barrier should be overcome by the driving force for coarsening. Assuming that the 2-D nucleus on the terrace surface is a circular disk of atomic height h and radius r, the free energy change associated with the formation of such a disk of the perimeter $2\pi r$ is given by

$$\Delta G = -\pi r^2 h \Delta G_d + 2\pi r \varepsilon, \tag{1}$$

where ε is the edge energy and ΔG_d is the driving force for nucleation. From this equation, the free energy of formation of a critical nucleus is

$$\Delta G_c = \frac{\pi \varepsilon^2}{h \Delta G_d}. \tag{2}$$

The 2-D nucleation rate has the following form:[28]

$$I = A \quad \exp\left(-\frac{\Delta G_c}{kT}\right), \tag{3}$$

where the pre-exponential factor A is mainly determined by the atomic jumping frequency and kT has the usual meaning. The factor A has the value in the range of $e^{50} \sim e^{65}$.[27,28] The 2-D nucleation rate has the exponential dependence on ΔG_c, which is again mainly determined

by ΔG_d and ε as shown in Eq. (2). It should be noted that the main conclusion of this paper comes from the exponential dependence of the 2-D nucleation rate on ΔG_c and is not affected by the choice of the pre-exponential factor, which differs in the range of $e^{50} \sim e^{65}$ between theories.[27,28]

In the case of Ostwald ripening, ΔG_d is provided by the difference in the capillary pressure or the chemical potential between grains of different size. According to the Wulff theorem, the ratio of the surface energy (γ_i) of each facet to the distance (R_i) from the center of the equilibrium shape to its facet is a constant. For simplicity, we assume that the equilibrium shape has only one type of face like cubic. Then, γ/R is a constant. In the mean field model, each grain interacts with the hypothetical grain of critical size (R^*) which does not grow nor dissolve at the given instant. The driving force for coarsening of the grain with the distance from the center of the equilibrium shape to the given facet, R, is expressed as

$$\Delta G_d = 2\gamma_{sl}\left(\frac{1}{R^*} - \frac{1}{R}\right) \tag{4}$$

where ΔG_d and γ_{sl} are the driving force per unit volume and the S/L energy of the given facet, respectively.

The growth rate for an angular grain with the center distance R can be obtained by simply multiplying the 2-D nucleation rate by the atomic height h. Therefore,

$$\frac{dR}{dt} = hA \quad \exp\left(-\frac{\Delta G_c}{kT}\right) = h\exp\left(\ln A - \frac{\pi\varepsilon^2}{2kTh\gamma_{sl}\left(\frac{1}{R^*} - \frac{1}{R}\right)}\right) \tag{5}$$

However, the dissolution rate for an angular grain of the center distance R does not follow Eq. (5). Although the growth barrier can be high on the singular interface, the dissolution barrier is known to be negligible and tends to be diffusion-controlled.[27] The reason is that each corner of the angular grain can act as a kink site for dissolution. Once dissolution starts from the corner and proceeds along the edge, the ledge continues to be generated. Therefore, the growth and the dissolution kinetics are not symmetrical for the angular grains. For this reason, the critical size tends to be much smaller than the average size. This is in contrast with the case of diffusion-controlled coarsening, where the critical size is equal to the average size. The dissolution of angular grains is regarded as being diffusion-controlled. Therefore, the dissolution rate for the grain with the center distance R is expressed as

$$\frac{dR}{dt} = \frac{D_f C_o \gamma_{sl} V_m^2}{kT}\frac{1}{R}\left(\frac{1}{R^*} - \frac{1}{R}\right), \tag{6}$$

where D_f and C_o represent diffusivity and solubility of the solute, respectively.

We should then consider mass conservation. At a given instant, the growth flux should be equal to the dissolution flux as expressed by the following equation:

$$-\int_0^{R_k} R^2\left(\frac{dR}{dt}\right)dt = \int_{R_k}^{Ri} R^2\left(\frac{dR}{dt}\right)dt \tag{7}$$

Eqs. (5), (6) and (7) have to be solved simultaneously.

For the numerical solution, the initial grain size distribution needs to be defined. The initial number of grains was 1000; the size of individual grains was determined by generating the random number having a Gaussian distribution with an arbitrary average and standard deviation. Typically, the average size was 0.3 μm with a standard deviation of 0.2. The numerical solution is for two-dimensional grains. There was no basic difference in the physical meaning of the calculation results between simulations of two-dimensional and three-dimensional grains except the amount of a material flux which is needed for growth. Three-dimensional grains needed a larger flux to grow to the same size as two-dimensional grains.

The integral form of Eq. (7) is changed to the summation as follows;

$$-\sum_0^k R_i\left(\frac{\Delta R_i}{\Delta t}\right)_{dissolve}\Delta t = \sum_k^{1000} R_i\left(\frac{\Delta R_i}{\Delta t}\right)_{grow}\Delta t. \tag{8}$$

In solving differential equations of Eqs. (5) and (6), the algorithm of Runge–Kutta order 4 was used. At each time step (Δt), a new R^* by binary search was determined, which satisfies the mass conservation of Eq. (8). With each new R^*, the incremental radius of each grain for the next step was determined from Eqs. (5) and (6). Δt of 0.01 was sufficient for accuracy; the smaller value of Δt did not change the result.

In order to examine the validity of our numerical approach, the diffusion-controlled coarsening was also solved by the same numerical procedure and compared the result with the analytic solution by LSW[2,3]. For the time step of 1000, the average size of the grains increased to $\sim$1.5 times as large as that of the initial grains. Normally, the iteration was done for the time step of 1000. The numerical solution was obtained as the numerical data for the radius of each grain after the given time step. In the case of diffusion-controlled coarsening, overlapping of the diffusion field was not considered. As a result, the solid fraction is small enough to avoid overlapping of the diffusion field, as was the assumption of the LSW theory.[2,3] In order to distinguish between diffusion-controlled and 2-D nucleation-controlled coarsening, the grains were displayed as spheres and squares, respectively.

For visualization of the data, the numerical data for the radius of each grain are graphically displayed. They are randomly distributed as white grains on the dark matrix but overlapping between grains was avoided. Since they were distributed in an arbitrary area, the volume fraction of the solid grains in the display lacks in physical meaning. The numerical solution for diffusion-controlled coarsening is valid under the condition that the volume fraction of solid grains is small enough to avoid overlapping of the diffusion field. Therefore, the volume fraction of the solid grains in the display of Figs. 1 and 4 is overestimated. However, the numerical solution for interface-controlled coarsening is valid regardless of the volume fraction of solid grains because the kinetics for interface-controlled coarsening is not affected by the diffusion distance between grains.

3. Results and discussion

Fig. 1(a) and (b) are the displays of the numerical data for diffusion-controlled coarsening after zero and 1000 steps, respectively. For the calculations, the initial average grain size and the standard deviation of the size distribution are taken to be 0.3 and 0.2 μm, respectively, and the temperature of 1300 K is assumed. On the other hand, $D_f = 10^{-3}$ m^2/s, $C_o = 1$ at.%, and $\gamma_{sl} = 0.1$ J/m^2 are used, which are typical values, except D_f, in liquid-phase sintered materials. The excessive D_f value is chosen in order to accelerate particle coarsening and to minimize the computation time. As shown in Fig. 1, coarsening is uniform and typical of diffusion-controlled growth of spherical grains. The growth rate of the critical size follows the cubic growth law and the grain size distribution normalized by the critical size does not change with time after a short period of an initial non-steady state. All these behaviors are in agreement with the analytical solution of the LSW theory, confirming the validity of this numerical approach.

Fig. 2(a) and (b) are the displays of the coarsening by 2-D nucleation after zero and 1000 steps, respectively. The parameters used are the same as those in Fig. 1. The additional parameter is the edge energy ε. In order for the edge energy to have the same unit as the interface energy, it should be divided by the edge height h. The maximum value that ε/h can have is the interface energy, which is the case at 0 K.[38,39] As the temperature increases, the edge energy decreases. At the temperature of interface roughening, it becomes zero.[40] Thus, the edge energy for the rough interface of the spherical grains is zero. In this calculation, it is assumed that ε/h of angular grains is equal to 0.2 γ_{sl} at the sintering temperature of 1300 K unless mentioned otherwise. In contrast with Fig. 1(b), one exceptionally large grain

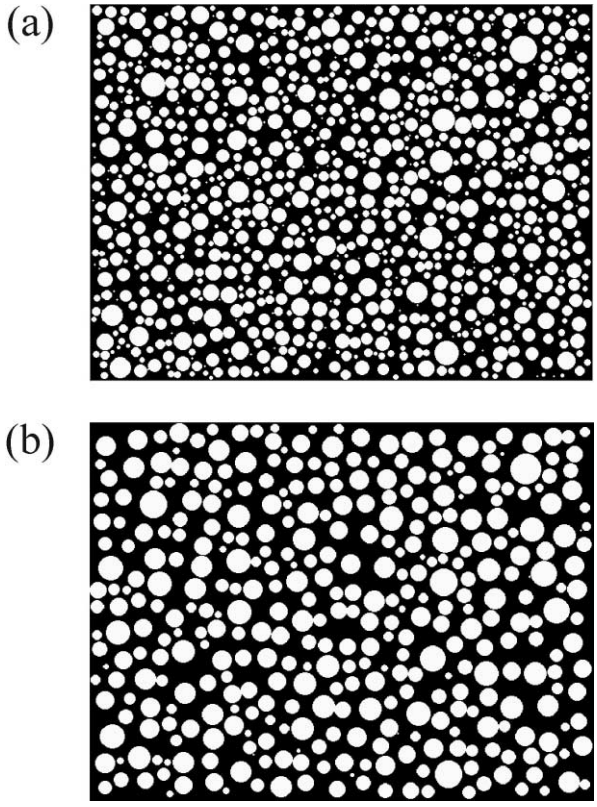

Fig. 1. Microstructural display of the numerical solution of diffusion-controlled coarsening: (a) after zero time step and (b) after 1000 time steps.

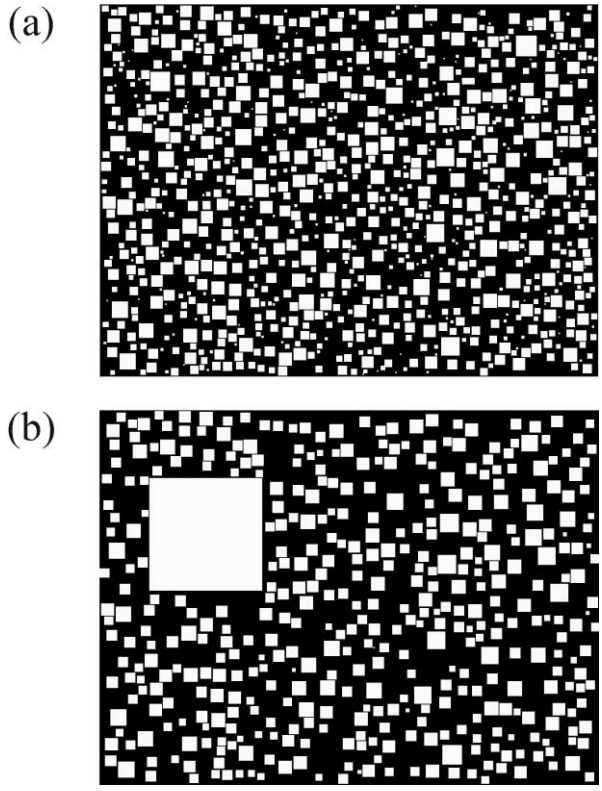

Fig. 2. Microstructural display of the numerical solution of 2-D nucleation-controlled coarsening: (a) after zero time step and (b) after 1000 time steps.

appears in Fig. 2(b), as is often the case of the real system of angular grains. In other words, AGG took place in Fig. 2(b).

The evolution of AGG in Fig. 2(b) is a direct result of the coarsening by 2-D nucleation, for which no artificial assumption intended for AGG was made. This result implies that AGG of angular grains dispersed in the liquid phase should be induced naturally by 2-D nucleation controlled coarsening. This is in agreement with the experimental observation that AGG occurs exclusively in the systems with angular grains. In addition to the visual display of AGG in Fig. 2(b), 2-D nucleation-controlled coarsening was tested with the other criteria for AGG. The following inequality is often used as a criterion for AGG.[41,42]

$$\frac{d(R_{max}/R_{ave})}{dt} > 0, \tag{9}$$

where R_{max} and R_{ave} represent the maximum and the average size of grains, respectively. Instead of R_{ave}, the critical size can be used. Based on the numerical solution, the size ratio of the largest to the average grain is plotted against the time step in Fig. 3(a). For comparison, the case for diffusion-controlled coarsening is plotted in Fig. 3(b). Fig. 3(a) shows that the ratio increases monotonically, satisfying the condition for AGG given by Eq. (9) all the way through the given time interval. On the other hand, Fig. 3(b) shows that the ratio decreases and ultimately reaches $R_{max}/R_{ave} \approx 2$ as expected from diffusion-controlled coarsening.[1]

Previously, AGG was attributed to the size advantage of the initially large grains, which are 4 to 5 times larger than the average size, because these grains have the large driving force.[43] This hypothesis can be treated in our numerical solution by adding an arbitrary large grain to the initial size distribution. The results between diffusion-controlled and 2-D nucleation-controlled coarsening were compared. For this purpose, one grain 10 times as large as the average of the initial grains was artificially added. It should be reminded that the size of the other initial grains is determined by the random number generation with some constraints mentioned earlier.

Fig. 4(a) and (b) show the display of the numerical data, respectively, before and after 1000 iterations for diffusion-controlled coarsening. In Fig. 4(b), the largest grain did not grow markedly compared to the other grains. The growth rate of the maximum grain normalized by the average size was negative all the way through the given time interval, not satisfying Eq. (9). On the other hand, Fig. 5(a) and (b) show the display, respectively, before and after 1000 iterations for the case of 2-D nucleation-controlled coarsening. The growth rate of the largest grain is higher than that of matrix grains so that AGG characteristics become more pronounced. The growth rate of the maximum grain normalized by the average size was positive all the way through the given time interval, satisfying Eq. (9). These analyses indicate that the size advantage cannot induce AGG if the coarsening kinetics are diffusion-controlled. At the same time the size advantage would be pronounced if the coarsening kinetics is 2-D nucleation controlled. Thus, exceptionally large grains can act as seeds for AGG in 2-D nucleation-controlled coarsening but they cannot in diffusion-controlled coarsening.

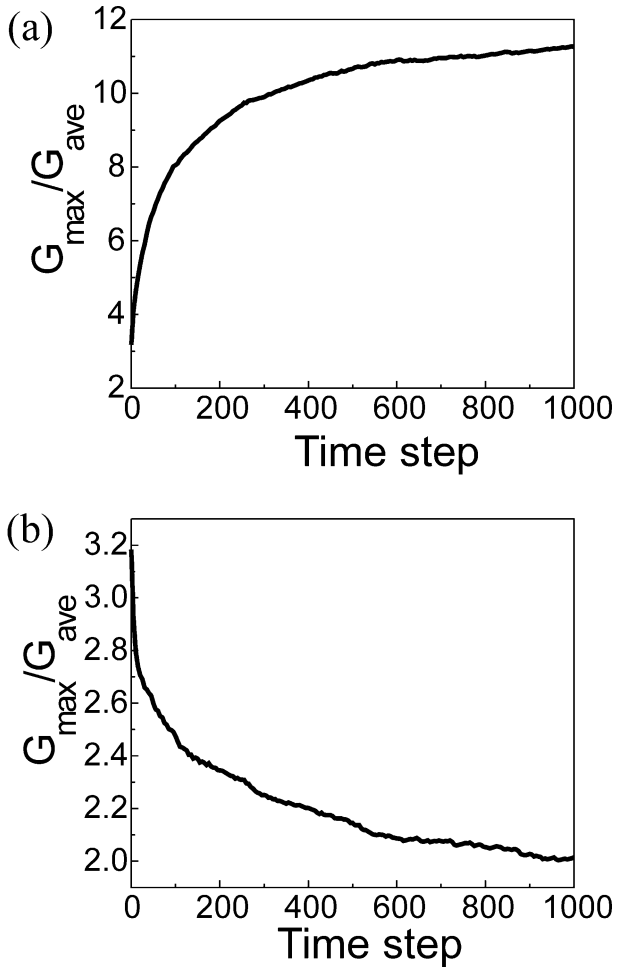

Fig. 3. Variation of the relative size of the largest grain to average grain with time: (a) 2-D nucleation-controlled and (b) diffusion-controlled coarsening.

It is well known that the nanometer size powder has a stronger tendency for AGG than micron sized powder.[18,44] For example, the nanometer size WC powder has much stronger tendency for AGG in the Co-rich liquid matrix than the micron size powder,[44] the fact of which has discouraged the development of nanometer size powder. Generally, the smaller the powder size, the more enhanced is AGG of the angular grains dispersed in the liquid matrix. Thus, the initial size effect on the coarsening behavior by 2-D nucleation was examined. The graphical displays of the results when the initial average size is 0.3 and 1 μm after 1000 iteration are shown in Fig. 6(a) and (b), respectively.

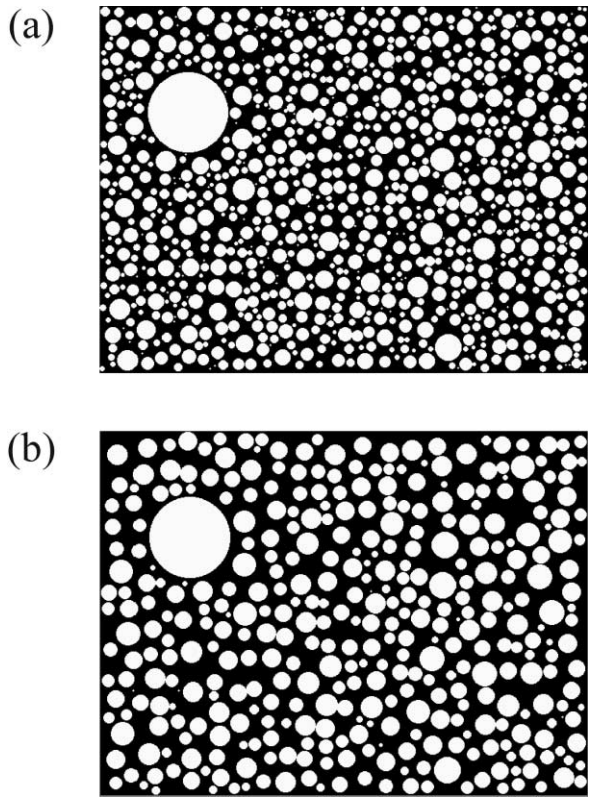

Fig. 4. Microstructural display of the numerical solution of a seeding effect on diffusion-controlled coarsening: (a) after zero time and (b) after 1000 time steps.

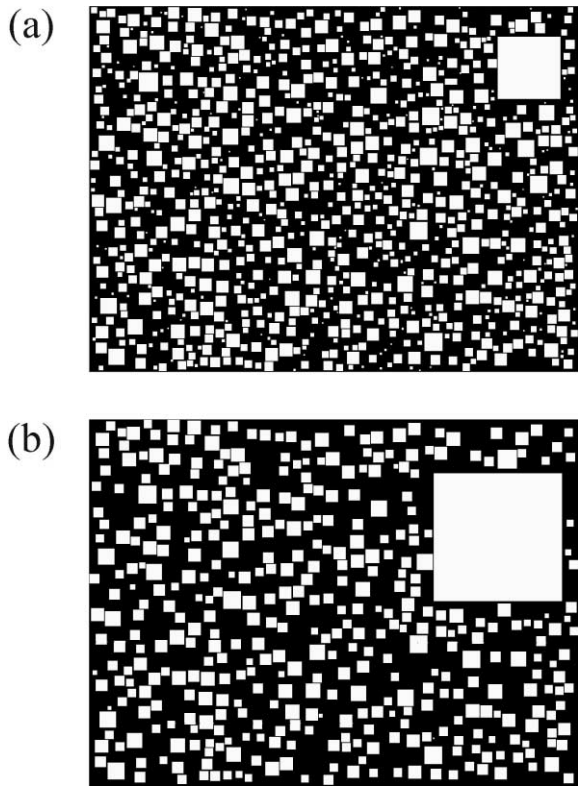

Fig. 5. Microstructural display of the numerical solution of a seeding effect for 2-D nucleation-controlled coarsening: (a) after zero time and (b) after 1000 time steps.

For the edge energy of 0.2 γ_{sl}, the grains of initial average 0.3 μm show distinctive AGG in Fig. 6(a) while those of 1 μm do not [Fig. 6(b)]. Besides, the grains of 1 μm average do not grow. This is because the capillary driving force provided by the average grains of 0.3 μm is high enough to trigger 2-D nucleation but that by the average grains of 1 μm is not. It should be noted that if edge energy is changed, the average grain size triggering 2-D nucleation is also changed. These results of the numerical solution are in agreement with the previous experimental observation by Park et al.[11] that the submicron size WC powder induced AGG in the Co-rich liquid matrix while the micron size WC did not. In reality, although the micron size WC grains did not show AGG, the grains underwent normal coarsening at a very low rate after extensive heat treatment. In this case, the grains are expected to grow by the spiral mechanism of screw dislocations at a low rate.

The analyses made hitherto indicate that coarsening by 2-D nucleation can induce AGG. Thus, the parameters that affect the 2-D nucleation rate in Eq. (5) would be important in inducing AGG. These parameters are the grain size, the temperature, the edge energy and the S/L interface energy. In Fig. 6, the effect of grain size was shown. Increasing the temperature will enhance the 2-D nucleation rate but decrease the edge energy and the S/L energy.[38,39] So the effect of temperature should be interpreted with caution. Decreasing the edge energy will increase the 2-D nucleation rate and will enhance AGG. Eq. (6) also indicates that for the given edge energy, increasing the S/L energy will increase the 2-D nucleation rate and enhance AGG. These effects of the edge energy and the S/L energy were confirmed by the numerical solution.[33]

In Fig. 7, the variation of the growth and dissolution rate as a function of the grain size normalized by the critical size was shown. The negative and positive values of the ordinate indicate dissolution and growth, respectively. The critical size, which neither grows nor dissolves, corresponds to the radius intercepting the abscissa. As shown in Fig. 7(a), the maximum growth rate for diffusion-controlled coarsening takes place at twice the critical size as reported previously.[1] For 2-D nucleation-controlled coarsening in Fig. 7(b), however, there is no maximum but the growth rate increases exponentially with increasing size. It should be noted that the ordinate of Fig. 7(b) is 100 times larger in scale than that of Fig. 7(a). In reality, the growth rate by 2-D nucleation cannot be higher than the ideal growth rate of the rough interface because of kinetic roughening.[40] The exponential dependence of the growth rate by 2-D nucleation on the grain size seems responsible for AGG.

The exponential dependence of the growth rate on the grain size not only provides the high growth rate for the

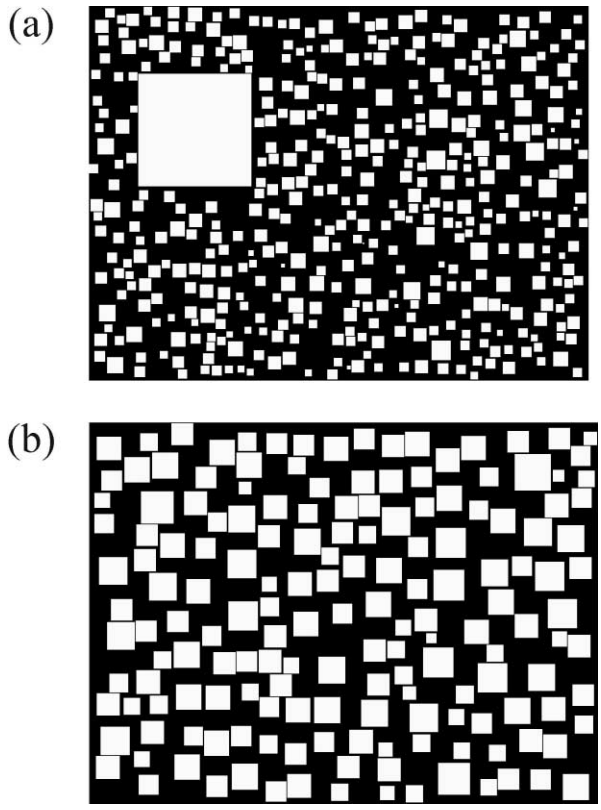

Fig. 6. Microstructural display of the numerical solution for 2-D nucleation-controlled coarsening with two difference sizes of an initial average particle after 1000 time steps; (a) 0.3 μm and (b) 1 μm.

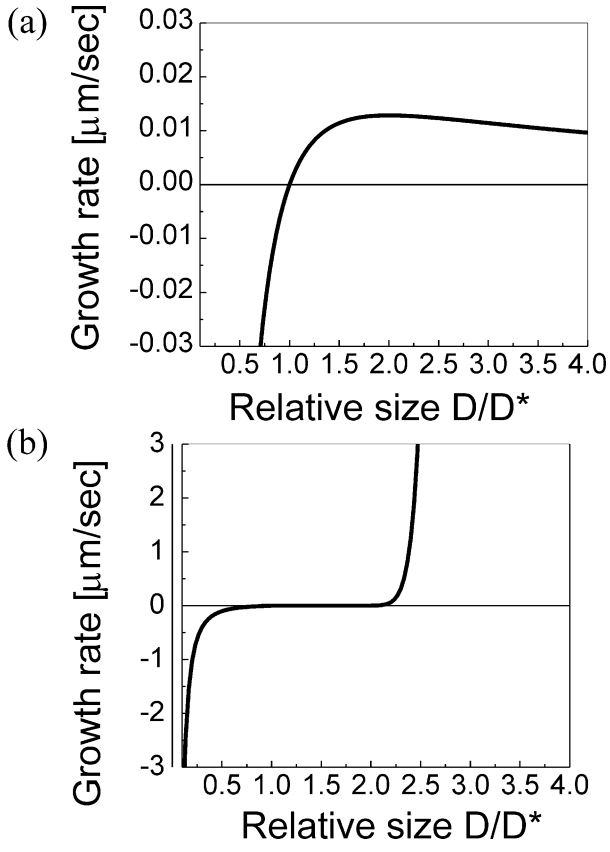

Fig. 7. Dependence of the growth rate on the relative size for (a) diffusion-controlled and (b) 2-D nucleation-controlled coarsening.

largest grain but also suppresses the growth of the other grains. Most of the grains, which are larger than the critical size and therefore have the driving force for growth, will not grow at all because their driving force is not large enough to trigger 2-D nucleation. Due to such suppression of the growth of the other grains, the high capillary driving force will be maintained. Because of this, the largest grain after AGG of angular grains can grow with a higher rate than that of the largest grain in the diffusion-controlled coarsening despite that the interface of the rough interface has always the higher mobility than that of the singular interface. This aspect can be examined as follows.

Comparing the size of the maximum grains between Figs. 2 and 3, the maximum grain size for 2-D nucleation-controlled coarsening is much larger than that for diffusion-controlled coarsening. This means that the growth rate of the former has been larger than that of the latter ($v_{2\text{-D}} >> v_{\text{diff}}$). The growth rate is usually expressed by the product of the mobility and the driving force as,

$$v = \frac{\mathrm{d}r}{\mathrm{d}t} = M\Delta G \tag{10}$$

Strictly speaking, M in Eq. (10) is not a constant but depends on the driving force as shown in Eqs. (5) and (6). Mobility of the rough interface undergoing diffusion-controlled coarsening is always higher than that of the singular interface undergoing 2-D nucleation-controlled coarsening regardless of the magnitude of the driving force ($M_{2\text{-D}} < M_{\text{diff}}$). The mobility of the singular interface will increase with the driving force and eventually has the same mobility as the rough interface, which corresponds to the kinetic roughening.[40] Considering $v_{2\text{-D}} >> v_{\text{diff}}$ and simultaneously $M_{2\text{-D}} < M_{\text{diff}}$, the driving force for coarsening of angular grains must be much larger than that of spherical grains, that is $\Delta G_{2\text{-D}} >> \Delta G_{\text{diff}}$. Since the driving force for coarsening is mainly determined by the critical size as shown in Eq. (1), the critical size for 2-D nucleation-controlled coarsening must be maintained to be smaller than that for diffusion-controlled coarsening.

These aspects can be seen in Fig. 8, where the critical radii were plotted against the time step for both cases. The average sizes for both cases were also drawn as dashed lines for comparison. However, in the case of diffusion-controlled coarsening, the critical size coincides exactly with the average size. In contrast, in the case of 2-D nucleation-controlled coarsening, the critical size is much smaller than the average size in all the time steps. This difference is related to the asymmetry in the dissolution and the growth rates. As mentioned

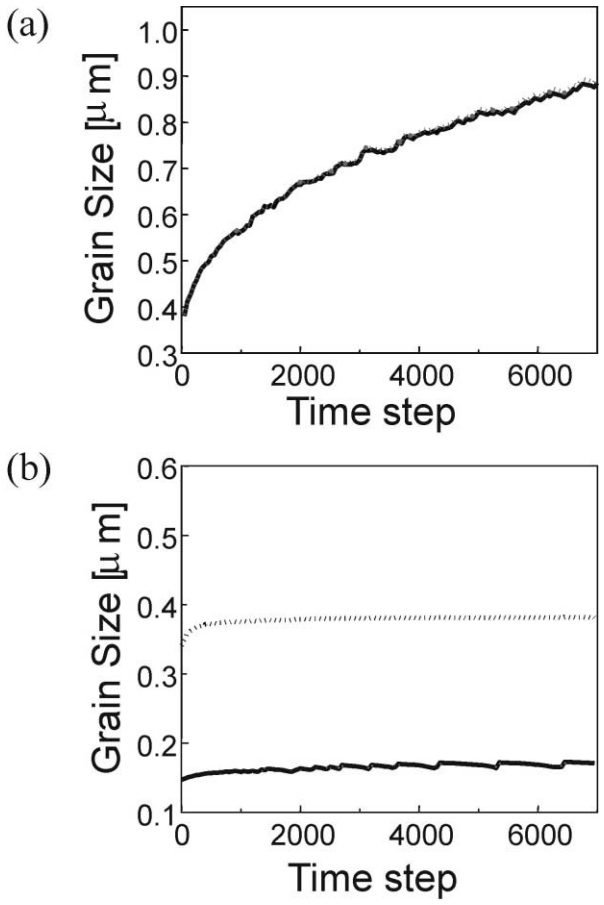

Fig. 8. Variation of the critical (solid line) and average (dashed line) sizes with time: (a) diffusion-controlled and (b) 2-D nucleation-controlled coarsening.

earlier, we assumed that dissolution of the angular grains is diffusion-controlled and the growth is 2-D nucleation-controlled. In other words, the dissolution rate is much faster than the growth rate.

On the other hand, it is known that the grain of the singular interface grows by both mechanisms of screw dislocation and 2-D nucleation.[27,28] In the real system with angular grains, both mechanisms will proceed in parallel with the faster one dominating. It is known that at the low driving force where the rate of 2-D nucleation is negligible, the growth by screw dislocation is dominant while at the high driving force, where the rate of 2-D nucleation is appreciable, the growth by 2-D nucleation is dominant.[27,28] According to our numerical approach, growth by screw dislocation did not induce AGG.[33]

As mentioned earlier, the growth rate by 2-D nucleation cannot be higher than the ideal growth rate of the rough interface because of kinetic roughening.[40] This kinetic roughening was not considered in this simulation. As a result, only one AGG grain tends to grow in Figs. 2 and 6. If the kinetic roughening is implemented in the simulation, a few grains undergo AGG, which describes more realistic situations.[45]

In real systems of liquid phase sintering of angular grains with a singular interface, the situation is much more complex than the assumptions made in this study. In some cases, the amount of a liquid phase is so small that it exists as thin films between grains. Besides, most grains are in contact each other with grain boundaries or liquid films in between. In such a case, it is not sure whether the assumption of a mean field in the present simulation is valid or not. However, the assumption of a mean field has a great advantage in that the complex phenomenon of coarsening can be simply formulated and be solved analytically or numerically. The present simulation may provide a pathway to more advanced treatments considering more realistic situations. Even in the case of diffusion-controlled coarsening, the modified LSW theory[4] dealing with more realistic cases of appreciable or large volume fraction of the second phase with overlapping diffusion field was based on the LSW theory[2,3] and on the mean field assumption.

Although the present analysis is more applicable to AGG of the system with an appreciable amount of liquid phase such as the WC–Co system,[11,37] some experimental results in the $BaTiO_3$ systems with a very small amount of liquid phase[34,36,46,47] could be successfully approached by the concept of the 2-D nucleation-controlled coarsening. In this system, the grains with a double twin grow exclusively over other grains. The double twin makes the persistent re-entrant edge, which provides the site of a much lower nucleation barrier than that on the terrace. Using seed grains with a double twin, Yoo et al.[34] and Lee et al.[46] could grow a single crystal of $BaTiO_3$ as large as $1\times1\times1$ cm^3. The re-entrant edge can also be made by the grain boundary between grains in contact. Choi et al.[48] clearly showed the growth advantage by the grain boundary re-entrant edge in the liquid phase sintering of TaC–TiC–Ni Cermets. Although the effect of re-entrant edge on AGG was not treated in the present numerical approach, the exclusive growth of grains with a re-entrant edge can be treated easily by the concept of coarsening limited by 2-D nucleation.[33]

4. Conclusions

Coarsening of angular grains by 2-D nucleation was numerically analyzed. The result showed that AGG takes place with the realistic values of the related parameters. AGG of angular grains by 2-D nucleation growth is attributed to the fact that a high driving force for coarsening is maintained because the growth of most of grains is suppressed. The flux for growth is concentrated on only a few grains, which are large enough to trigger 2-D nucleation.

Acknowledgements

This work was supported by the Creative Research Initiatives Program of Korea Ministry of Science and Technology.

References

1. Greenwood, G. W., The growth of dispersed precipitates in solutions. *Acta Metall.*, 1956, **4**, 243–248.
2. Lifshitz, I. M. and Slyozov, V. V., The kinetics of precipitation from supersaturated solid solutions. *J. Phys. Chem. Solids*, 1961, **19**, 35–50.
3. Wagner, C., Ostwald ripening theory. *Ber. Bunsenges. Phys. Chem.*, 1961, **65**, 581–591.
4. Ardell, A. J., The effect of volume fraction on particle coarsening: theoretical consideration. *Acta Metall.*, 1972, **20**, 61–71.
5. Nakashima, S., Takashima, K. and Harase, J., Effect of thickness on secondary recrystallization of Fe–3%Si. *Acta Metall. Mater.*, 1994, **42**, 539–547.
6. Hwang, N. M., Lee, S. B., Han, C. H. and Yoon, D. Y., Effect of solid-state wetting along grain boundary or triple junction on abnormal grain growth. In *Proceedings of Grain Growth in Polycrystalline Materials III*, ed. H. Weiland, B. L. Adams, and A. D. Rollet. The Minerals, Metals & Materials Society, 1998, pp. 327–332.
7. Jackson, K. A., *Liquid Metals and Solidification*. American Society for Metals, Ohio, 1958.
8. Kang, S. S. and Yoon, D. N., Kinetics of grain coarsening during sintering of Co–Cu and Fe–Cu alloys with low liquid contents. *Metall. Trans.*, 1982, **13A**, 1405–1411.
9. Kang, T. K. and Yoon, D. N., Coarsening of tungsten grains in liquid nickel-tungsten matrix. *Metall. Trans.*, 1978, **9A**, 433–438.
10. Kang, S. J. L., Kaysser, W. A., Petzow, G. and Yoon, D. N., Elimination of pores during liquid phase sintering of Mo–Ni. *Powder Metall.*, 1984, **27**, 97–100.
11. Park, Y. J., Hwang, N. M. and Yoon, D. Y., Abnormal growth of faceted (WC) grains in a (Co) liquid matrix. *Metall. Mater. Trans.*, 1996, **27A**, 2809–2819.
12. Warren, R. and Waldron, M. B., Microstructural development during the liquid-phase sintering of cemented carbides. I. wettability and grain contact. *Powder Metall.*, 1972, **15**, 166–180.
13. Prochanzka, S., Dole, S. L. and Hejna, C. I., Abnormal grain growth and microcracking in boron carbide. *J. Am. Ceram. Soc.*, 1985, **68**, C–235-C-236.
14. Heuer, A. H., Fryburg, G. A., Ogbuji, L. U., Mitchell, T. E. and Shinozaki, S., $\beta \rightarrow \alpha$ transformation in polycrystalline SiC: I. *microstructural aspects. J. Am. Ceram. Soc.*, 1978, **61**, 406–412.
15. Song, H. S. and Coble, R. L., The origin and growth kinetics of plate-like abnormal grains in liquid-phase-sintered alumina. *J. Am. Ceram. Soc.*, 1990, **73**, 2077–2085.
16. Hennings, D. F. K., Janssen, R. and Reynen, P. J. L., Control of liquid phase-enhanced discontinuous grain growth in barium titanate. *J. Am. Ceram. Soc.*, 1987, **70**, 23–27.
17. Yoon, H.-H. and Kim, D.-Y., Effect of heating rate on the exaggerated grain growth during the sintering of Sr-hexaferrite. *Mater. Lett.*, 1994, **20**, 293–297.
18. Chol, G. R., Influence of milled powder particle size distribution on the microstructure and electrical properties of sintered Mn-Zn ferrites. *J. Am. Ceram. Soc.*, 1971, **54**, 34–39.
19. Fagan, J. G. and Amarakoon, V. R. W., Sol-gel coating of $YBa_2Cu_3O_{7-x}$ with TiO_2 for enhanced anisotropic grain growth. *J. Mater. Res.*, 1993, **8**, 1501–1509.
20. Jeong, I.-K., Kim, D.-Y., Khim, Z. G. and Kwon, S. J., Exaggerated grain growth during the sintering of Y–Ba–Cu–O superconductor ceramics. *Mater. Lett.*, 1989, **8**, 91–94.
21. Hong, S. H. and Messing, G. L., Anisotropic grain growth in diphasic gel-derived titania-doped mullite. *J. Am. Ceram. Soc.*, 1998, **81**, 1269–1277.
22. Kang, S. J. L. and Han, S. M., Grain growth in Si_3N_4 based materials. *MRS Bull.*, 1995, **20**, 33–37.
23. Rhee, S.-H., Lee, J. D. and Kim, D.-Y., Effect of heating rate on the exaggerated grain growth behavior of β-Si_3N_4. *Mater. Lett.*, 1997, **32**, 115–120.
24. Oh, U.-C., Chung, Y.-S., Kim, D.-Y. and Yoon, D. N., Effect of grain growth on pore coalescence during the liquid phase sintering of MgO–$CaMgSiO_4$ system. *J. Am. Ceram. Soc.*, 1988, **71**, 854–857.
25. Lee, D.-D., Kang, S.-J. L. and Yoon, D. N., Mechanism of grain growth and α-β transformation during liquid phase sintering of β'-sialon. *J. Am. Ceram. Soc.*, 1988, **71**, 803–806.
26. Han, S.-M. and Kang, S.-J. L., Comment on kinetics of β-Si_3N_4 grain growth in Si_3N_4 ceramics sintered under high nitrogen pressure. *J. Am. Ceram. Soc.*, 1993, **76**, 3178–3179.
27. Markov, I. V., *Crystal Growth for Beginners*. World Scientific Publishing Co. Ltd, Singapore, 1994.
28. Hirth, J. P. and Pound, G. M., *Condensation and Evaporation. . Progress in Materials Science*, 11. Pergamon Press Ltd, London, 1963.
29. Brice, J. C., *The Growth of Crystals from Liquids*. North-Holland, Amsterdam, The Netherlands, 1973.
30. Herring, C., Effect of change of scale on sintering phenomena. *J. Appl. Phys.*, 1950, **21**, 301–303.
31. Wynblatt, P. and Gjostein, N. A., Particle growth in model supported metal catalysts—I. Theory. *Acta Metall.*, 1976, **24**, 1165–1174.
32. Wynblatt, P., Particle growth in model supported metal catalysts-II. Comparison of experiment with theory. *Acta Metall.*, 1976, **24**, 1175–1182.
33. Kang, M.-K., *Numerical Analysis on the Growth of Solid Grains Dispersed in a Liquid Matrix*. PhD thesis, Seoul National University, Seoul, Korea, 1999.
34. Yoo, Y.-S., Kim, H. and Kim, D.-Y., Effect of SiO_2 and TiO_2 addition on the exaggerated grain growth of $BaTiO_3$. *J. Eur. Ceram. Soc.*, 1997, **17**, 805–811.
35. Kwon, S.-K., Hong, S.-H., Kim, D.-Y. and Hwang, N. M., Coarsening behavior of C_3S and C_2S grains dispersed in a clinker melt. *J. Am. Ceram. Soc.*, 2000, **83**, 1247–1252.
36. Kang, M.-K., Yoo, Y.-S., Kim, D.-Y. and Hwang, N. M., Growth of $BaTiO_3$ seed grains by the twin plane re-entrant edge mechanism. *J. Am. Ceram. Soc.*, 2000, **83**, 385–390.
37. Choi, K., Hwang, N. M. and Kim, D.-Y., Effect of VC addition on the microstructural evolution of WC–Co alloy: mechanism of grain growth inhibition. *Powder Metall.*, 2000, **43**, 168–172.
38. van Beijeren, H., Exactly solvable model for the roughening transition of a crystal surface. *Phys. Rev. Lett.*, 1977, **38**, 993–996.
39. Williams, E. D. and Bartelt, N. C. In *Handbook of Surface Science*, ed. W. N. Unertl. Elsevier Science, Amsterdam, 1996.
40. Bennema, P., Growth and morphology of crystals: integration of theories of roughening and Hartman–Perdok theory. In *Handbook of Crystal Growth,* Vol. 1A, Chapter 7. North-Holland, Amsterdam, The Netherlands, 1993.
41. Rios, P. R., Abnormal grain growth in pure materials. *Acta Metall.*, 1992, **40**, 2765–2768.
42. Rios, P. R., Abnormal grain growth in materials containing particles. *Acta Metall.*, 1994, **42**, 839–843.
43. Hillert, M., On the theory of normal and abnormal grain growth. *Acta Metall.*, 1965, **13**, 227–238.
44. Yang, J., Eun, K.-Y. and Kim, D.-Y., Formation of anomalous

large grains in WC-Co alloy observed by Co infiltration. *Powder Metall. Int*., 1986, **18**, 62–64.
45. Lee, J. O., Kang, M. K., Kim, D.-Y., Hwang, N. M. (in preparation).
46. Lee, H.-Y., Kim, J.-S. and Kim, D.-Y., Fabrication of $BaTiO_3$ single crystals using secondary abnormal grain growth. *J. Eur. Ceram. Soc*., 2000, **20**, 1595–1597.
47. Kang, M. K., Park, J. K., Kim, D.-Y. and Hwang, N. M., Effect of temperature on the shape and coarsening behavior of $BaTiO_3$ grains dispersed in a SiO_2-rich liquid matrix. *Mater. Lett*., 2000, **45**, 43–46.
48. Choi, K., Choi, J. W., Kim, D. Y. and Hwang, N. M., Effect of coalescence on the grain coarsening during liquid-phase sintering of TaC–TiC–Ni cermets. *Acta Mater*., 2000, **48**, 3125–3129.